

# 1 Anthropogenic aerosol forcing under the Shared Socioeconomic Pathways

2 Marianne T. Lund<sup>\*,1</sup>, Gunnar Myhre<sup>1</sup>, Bjørn H. Samset<sup>1</sup>

3 1 CICERO Center for International Climate Research, Oslo, Norway

4 \*Corresponding author: Marianne T. Lund, m.t.lund@cicero.oslo.no

5

## 6 Abstract

7 Emissions of anthropogenic aerosols are expected to change drastically over the coming decades,  
8 with potentially significant climate implications. Using the most recent generation of harmonized  
9 emission scenarios, the Shared Socioeconomic Pathways (SSPs) as input to a global chemistry  
10 transport and radiative transfer model, we provide estimates of the projected future global and  
11 regional burdens and radiative forcing of anthropogenic aerosols under three contrasting pathways  
12 for air pollution levels: SSP1-1.9, SSP2-4.5 and SSP3-7.0. We find that the broader range of future  
13 air pollution emission trajectories spanned by the SSPs compared to previous scenarios translates  
14 into total aerosol forcing estimates in 2100 relative to 1750 ranging from  $-0.04 \text{ W m}^{-2}$  in SSP1-1.9  
15 to  $-0.51 \text{ W m}^{-2}$  in SSP3-7.0. Compared to our 1750-2015 estimate of  $-0.55 \text{ W m}^{-2}$ , this shows that  
16 depending on the success of air pollution policies and socioeconomic development over the  
17 coming decades, aerosol radiative forcing may weaken by nearly 95% or remain close to the pre-  
18 industrial to present-day level. In all three scenarios there is a positive forcing in 2100 relative to  
19 2015, from  $0.51 \text{ W m}^{-2}$  in SSP1-1.9 to  $0.04 \text{ W m}^{-2}$  in SSP3-7.0. Results also demonstrate significant  
20 differences across regions and scenarios, especially in South Asia and Africa. While rapid  
21 weakening of the negative aerosol forcing following effective air quality policies will unmask  
22 more of the greenhouse gas-induced global warming, slow progress on mitigating air pollution  
23 will significantly enhance the atmospheric aerosol levels and risk to human health in these regions.  
24 In either case, the resulting impacts on regional and global climate can be significant.

25

## 26 1 Introduction

27 Understanding the contribution of aerosols and other short-lived climate forcers to the total  
28 anthropogenic radiative forcing (RF) is becoming increasingly important considering the  
29 ambitious goals of the Paris Agreement. Under scenarios compliant with keeping global warming  
30 below  $1.5^\circ\text{C}$ , global greenhouse gas emissions must generally be reduced to net zero by the middle  
31 of the century, placing added focus on the evolution and relative importance of emissions of other  
32 climate-relevant substances for the net future climate impact (IPCC, 2018). Additionally, aerosols  
33 play a key role in shaping regional climate and environment, by modulating clouds, circulation  
34 and precipitation and air quality. In South and East Asia, currently the largest emission source  
35 regions, air pollution is one of the major health risks, estimated to have been responsible for 1.2  
36 million deaths in 2017 in India alone (Balakrishnan et al., 2019). In the same region, aerosols may  
37 have masked up to  $1^\circ\text{C}$  of surface warming (Samset, 2018), and the sensitivity of the regional  
38 climate to reductions in aerosol emissions has been found to be high (Samset et al., 2018a).

39 Several long-term scenarios for air pollutant emissions exist. Among the most recent examples are  
40 the Representative Concentration Pathways (RCPs) (Granier et al., 2011). The RCPs formed the  
41 basis for the Coupled Model Intercomparison Project Phase 5 (CMIP5) and have been used in a  
42 number of studies to estimate the potential impact of future changes in aerosols on air quality and  
43 health (e.g., Li et al., 2016; Partanen et al., 2018; Silva et al., 2016), radiative forcing and  
44 temperature (e.g., Chalmers et al., 2012; Shindell et al., 2013; Szopa et al., 2013; Westervelt et al.,  
45 2015) and precipitation and other climate variables (Nazarenko et al., 2015; Pendergrass et al.,  
46 2015; Rotstayn et al., 2014).

47 The RCPs were developed to span a range of climate forcing levels and were not associated with  
48 specific socio-economic narratives. The RCPs generally reflect the assumption that air quality  
49 regulations will be successfully implemented globally (Rao et al., 2017). As a result, emissions of  
50 aerosols and aerosol precursors are projected to decline rapidly in all scenarios, even under high  
51 forcing and greenhouse gas emission levels. However, despite efforts to control pollutant  
52 emissions, ambient air quality continues to be a major concern in many parts of the world. Global  
53 emissions of black and organic carbon (BC, OC) have increased rapidly over recent decades  
54 (Hoesly et al., 2018). Global emissions of sulfur dioxide (SO<sub>2</sub>) have declined, driven by legislation  
55 in Europe and North America, the collapse of the former Soviet Union and, more recently, air  
56 quality policies in China (Li et al., 2017; Zheng et al., 2018). However, in other regions of the  
57 world, most notably South Asia, SO<sub>2</sub> emissions continue to be high and are increasing. The aerosol  
58 and precursor emissions in the RCPs are generated following the assumption that economic growth  
59 leads to decreased emissions, i.e., following the so-called environmental Kuznets curve. The real-  
60 world representativeness of this relationship has, however, been questioned (Amann et al., 2013;  
61 Ru et al., 2018). Combined with the slow observed progress on alleviating air pollution, the  
62 question of whether previous projections of future emissions are too optimistic in terms of  
63 pollution control arises. More recent scenario development has included alternative assumptions  
64 to better understand the mechanisms and interlinkages with reference scenarios and climate policy  
65 co-benefits (Chuwah et al., 2013; Rao et al., 2013; Rogelj et al., 2014). These provide a wider  
66 range of possible developments but are still largely independent of underlying narratives.

67 To provide a framework for combining future climate scenarios with socioeconomic development,  
68 the Shared Socioeconomic Pathways (SSPs) (O'Neill et al., 2014) were produced. The SSPs  
69 provide five narratives for plausible future evolution of society and natural systems in the absence  
70 of climate change and combine these with seven different climate forcing targets using integrated  
71 assessment modeling, building a matrix of emission scenarios with socioeconomic conditions on  
72 one axis and climate change on the other. Associated narratives for air pollution emissions have  
73 been developed, representing three levels of pollution control (strong, medium and weak) based  
74 on characteristics of control targets, rate of implementation of effective policies and technological  
75 progress (Rao et al., 2017). These pollution storylines are then matched with SSP baseline marker  
76 and climate mitigation narratives. In SSP1 and SSP5, the combination of strong pollution control,  
77 high level of development and increasing health and environmental concerns result in reduced air

78 pollution emission levels in the medium to long term. A similar, but slower development is seen  
79 under medium control and medium challenges to societal development (SSP2), whereas with weak  
80 control and greater inequality in SSP3 and SSP4 progress is slowed and regionally fragmented.  
81 The numerous drivers influencing future development results in a broad range in projected  
82 emissions, between baseline marker scenarios and for a given SSP depending on the climate  
83 mitigation targets, generally with the highest emissions in SSP3, followed by SSP4, and the lowest  
84 in SSP1 or SSP5 (Rao et al., 2017).

85 Here we use three of the SSP scenarios as input to a global chemical transport model and offline  
86 radiative transfer calculations (Sect. 2) in order to quantify the future evolution of aerosols under  
87 strong, medium and weak air pollution control. We present results for both global and regional  
88 developments in aerosol loadings and radiative forcing (Sec. 3) and discuss implications of the  
89 findings in the context of previous generation emission scenarios and outlooks for more detailed  
90 studies of the wider climate implications of potential air quality policies (Sect. 4). Conclusions are  
91 given in Sect.5.

92

## 93 2 Method

94 Atmospheric concentrations of aerosols are simulated with the OsloCTM3 (Søvde et al., 2012).  
95 The OsloCTM3 is a global, offline chemistry-transport model driven by meteorological forecast  
96 data from the European Center for Medium Range Weather Forecast (ECMWF) OpenIFS model.  
97 Here the model is run in a  $2.25^\circ \times 2.25^\circ$  horizontal resolution, with 60 vertical levels (the uppermost  
98 centered at 0.1 hPa). The present-day aerosol distributions simulated by the OsloCTM3 were  
99 recently documented and evaluated by Lund et al. (2018). We refer to the same paper for detailed  
100 descriptions about the aerosol modules and treatment of scavenging and transport in the  
101 OsloCTM3. All simulations are performed with meteorological data for 2010. Lund et al. (2018)  
102 investigated the impact of meteorology on the simulated aerosol abundances using data for two  
103 years with opposite El Niño–Southern Oscillation (ENSO) index. Differences in global burden of  
104 up to 10% for some aerosol species were found, with occasional larger values in localized regions  
105 over the tropical Pacific and Atlantic Oceans.

106

107 Simulations with SSP air pollution emissions from fossil fuel, biofuel and biomass combustion are  
108 performed for the years 2015, 2020, 2030, 2050 and 2100, keeping the meteorology fixed. Nine  
109 emissions scenarios have been gridded and harmonized with the Community Emission Data  
110 System (CEDS) historical emissions (Gidden et al., 2019) and are available via Earth System Grid  
111 Federation (ESGF) by the Integrated Assessment Modeling Consortium (IAMC). Here, we use the  
112 IMAGE (van Vuuren et al., 2017) SSP1-1.9, MESSAGE-GLOBIOM (Fricko et al., 2017) SSP2-  
113 4.5 and AIM (Fujimori et al., 2017) SSP3-7.0 scenarios. SSP1-1.9 represents a pathway with  
114 strong air pollution control, low climate forcing level and low mitigation and adaptation challenges,  
115 while weak air pollution control, high climate forcing and high mitigation and adaptation  
116 challenges characterizes SSP3-7.0. SSP2-4.5 is an intermediate pathway. Air pollution emissions

117 in the remaining scenarios largely fall in the range between SSP1-1.9 and SSP3-7.0. Each  
118 simulation is run for 18 months, discarding the first six as spin-up. Natural emission sources (soil,  
119 ocean, biogenic organic compounds from vegetation) are kept at the present-day level and the data  
120 sets described in Lund et al. (2018). See Sect. 4 Discussion for comments on the potential  
121 implications of this choice.

122 Using the same model setup as in the present study, Lund et al. (2018) recently calculated the  
123 historical (1750-2014) evolution of aerosols following the Community Emission Data System  
124 (CEDS) inventory (Hoesly et al., 2018). The future projections from the present study are  
125 combined with this historical time series. Furthermore, whereas Lund et al. (2018) only assessed  
126 the direct aerosol RF, we here include an estimate of the radiative forcing due to aerosol-cloud  
127 interactions.

128 We calculate the instantaneous top-of-the atmosphere radiative forcing due to aerosol-radiation  
129 interactions (RFari) (Myhre et al., 2013b) using offline radiative transfer calculations with a multi-  
130 stream model using the discrete ordinate method (Stamnes et al., 1988). The same model has been  
131 used in earlier studies of RFari (Bian et al., 2017; Myhre et al., 2013a) with some small recent  
132 updates to aerosol optical properties (Lund et al., 2018). The radiative forcing of aerosol-cloud  
133 interactions (RFaci) (earlier denoted the cloud albedo effect or Twomey effect) is calculated using  
134 the same radiative transfer model. To account for the change in cloud droplet concentration  
135 resulting from anthropogenic aerosols, which alter the cloud effective radius and thus the optical  
136 properties of the clouds, the approach from Quaas et al. (2006) is used. This method has also been  
137 applied in earlier studies (Bian et al., 2017).

138

### 139 3 Results

140 In the following, we first document the future global emissions and abundances of aerosols,  
141 according to our three chosen SSP scenarios. We then show the resulting regional aerosol burden  
142 levels, and finally global and regional radiative forcing.

143 Figure 1a-d shows annual global emissions (fossil fuel, biofuel and biomass burning) of BC, OC,  
144 SO<sub>2</sub> and nitrogen oxides (NO<sub>x</sub>) from 1950 to 2100 in the CEDS inventory and the SSPs used in  
145 the present analysis. For comparison, we also include the RCP2.6 (van Vuuren et al., 2007),  
146 RCP4.5 (Smith & Wigley, 2006) and RCP8.5 (Riahi et al., 2007) 2015-2100 emissions. Total  
147 emissions excluding biomass burning are shown in Fig. S1. For all four species, the temporal  
148 evolution and difference between scenarios have similar characteristics. In SSP1-1.9, emissions  
149 are projected to decline from 2015. This decline is particularly rapid for BC and SO<sub>2</sub>, with  
150 emissions falling to around 25% of their 2015 levels already by 2040. For NO<sub>x</sub> and OC, emissions  
151 are projected to go down by around 80% by the end of the century. Apart from SO<sub>2</sub>, SSP3-7.0 sees  
152 an increase in emissions by towards the mid-21<sup>st</sup> century (by 10-20% above 2015 levels), followed  
153 by a decline back to, or slightly below the present-day by 2100. Emissions in SSP2-4.5 follow an  
154 intermediate pathway; a decline throughout the century, but less steep and with a higher end-of-

155 century levels than SSP1-1.9. As a result of the relatively similar underlying assumptions about  
156 the level of air pollution mitigation, the RCPs display much smaller spread and emissions fall  
157 throughout the century. All three RCPs generally lie between SSP1-1.9 and SSP2-4.5. There is  
158 also a decline in biomass burning emissions in SSP1-1.9 and SSP2-4.5, where emissions are  
159 around 30%-40% lower in 2100 compared to 2015. Rao et al. (2017) note that changes in biomass  
160 burning emissions are not necessarily driven by air pollution policies but can be linked to  
161 assumptions about the land-use sector in the respective integrated assessment models.

162 The rapidly decreasing anthropogenic emissions in SSP1-1.9 result in global total burdens (Fig.  
163 1e-h) of BC, primary organic aerosol (POA) and sulfate that are 30%, 45% and 60%, respectively,  
164 of the present-day level by 2100. Under this pathway, biomass burning sources become relatively  
165 more important over the century: fossil fuel and biofuel emissions constitute 70% of the total BC  
166 burden in 2015, but only 36% by 2100. Similar end-of-century changes are found under SSP2-4.5,  
167 but in this case the decline mainly occurs after 2050. In SSP3-7.0, the global aerosol burdens  
168 increase toward the mid-century followed by a small or negligible change to 2100 compared to  
169 2015. The global burden of nitrate is twice as high in 2100 compared to 2015 in SSP3-7.0. This is  
170 due to the combination of increased global ammonia (NH<sub>3</sub>) emissions (not shown here, see Gidden  
171 et al. (2019)), which are 30% higher by 2100, a small net change in NO<sub>x</sub> emissions and a decrease  
172 in SO<sub>2</sub> emissions, resulting in less competition for available ammonia by sulfate aerosols. The  
173 potentially more important role of nitrate aerosols under certain emission pathways has been  
174 documented in previous studies as well (Bauer et al., 2007; Bellouin et al., 2011). In SSP1-1.9 and  
175 SSP2-4.5, there is negligible net change in NH<sub>3</sub> emissions over the century, while NO<sub>x</sub> emissions  
176 decline, resulting in a lower burden also of nitrate. Figure 1i-j shows the simulated anthropogenic  
177 global-mean aerosol optical depth (AOD) and absorption aerosol optical depth (AAOD)  
178 (calculated as the difference between each year and the 1750 value, with meteorology and hence  
179 contribution from natural aerosols constant). The anthropogenic AOD falls from 0.026 in 2015 to  
180 0.0005 in 2100 in SSP1-1.9 and 0.006 in SSP2-4.5. These changes correspond to a reduction of  
181 the total AOD of 20% (15%) in 2100 in SSP1-1.9 (SSP2-4.5) from the present-day level of 0.13.  
182 In SSP3-7.0, the anthropogenic AOD increases by 12% to 2050 before returning approximately to  
183 its present-day value. Similar magnitude decreases in anthropogenic AAOD are found. The decline  
184 in anthropogenic AOD is stronger than implied by the burden changes. We note that the sulfate  
185 and nitrate burdens include also smaller contributions from natural (ocean and vegetation) sources  
186 that remain constant to 2100. In SSP1-1.9 we find a small, negative AAOD value in 2100. This  
187 results from emissions on BC and OC being lower in 2100 than in 1750. The stronger decline in  
188 anthropogenic AAOD relative to AOD in SSP1-1.9 is reflected in the total (anthropogenic and  
189 natural aerosols) Single Scattering Albedo (SSA) (Fig. 1k) which increases to above pre-1970s  
190 levels by mid-century and is notably higher than in SSP3-7.0 by the end of the century. As the  
191 mechanisms that link aerosol emissions to climate impacts are markedly different for scattering  
192 and absorbing aerosols (Ocko et al., 2014; Samset et al., 2016; Smith et al., 2018), this reduction  
193 highlights a need for regional studies of aerosol impacts that go beyond the total top-of-atmosphere  
194 effective radiative forcing.

195 The global-mean time series hide significant spatiotemporal differences in aerosol trends. Figure  
196 2 shows the time series of the BC and sulfate burdens, the two dominant species, averaged across

197 9 regions: North America (NAM), Europe (EUR), Russia (RBU), East Asia (EAS), South Asia  
198 (SAS), South East Asia (SEA), North Africa and the Middle East (NAF\_MDE), South Africa (SAF)  
199 and South America (SAM). The well-known geographical shift in historical emission is clearly  
200 reflected, where the largest aerosols loadings were located over North America, Europe and Russia  
201 in the 1970s and 80s, but later peaking over Asia. In the coming decades, South and East Asia will  
202 continue to experience the highest aerosol loadings under SSP2-4.5 and SSP3-7.0. Towards the  
203 end of the century North Africa and the Middle East are projected to experience levels similar to  
204 those in South and East Asia. Africa south of the Sahara is presently the third largest BC emission  
205 source region (Fig. S2). Under SSP3-7.0, anthropogenic (fossil and biofuel) emissions are  
206 projected to increase strongly over the century and the region surpasses East Asia as the largest  
207 source in 2100, although levels stay below current emission levels in China. Figure 2 shows that a  
208 slightly decreasing BC burden is projected over the region in all three SSPs. In this case, the  
209 increase in fossil fuel emissions is offset by a decrease in biomass burning emissions, which  
210 constitute a significant fraction of the total BC source here. Despite lower emissions in the latter  
211 region, BC burdens in SAF and NAF\_MDE are of the same order of magnitude. One reason for  
212 this is likely differing scavenging pathways, where aerosols are more effectively removed, and the  
213 atmospheric residence time is shorter, further south. Moreover, we note that the regionally  
214 averaged burden does not directly link to regional emissions, as they are also influenced by long-  
215 range transport. Using multi-model data from the Hemispheric Transport of Air Pollution (HTAP2)  
216 experiments, studies have demonstrated that while for most receptor regions, within-region  
217 emissions dominates, there are the important contribution from long-range transport from e.g.,  
218 Asia to aerosols over North America, Middle East and Russia (e.g., Liang et al., 2018; Stjern et al.,  
219 2016; Tan et al., 2018). Hence, the projected emission changes in this region can have far reaching  
220 impacts.

221 The radiative forcing of anthropogenic aerosols relative to 1750 is shown for the period 1950 to  
222 2100 in Fig. 3, for RFari, RFaci, and the total aerosol RF (RFtotal), separately. Results from the  
223 present study are complimented by results based on simulations from Lund et al. (2018) (see  
224 Methods) for the historical period. We calculate a net aerosol-induced RF in 2015, relative to 1750,  
225 of  $-0.55 \text{ W m}^{-2}$ , whereof  $-0.14 \text{ W m}^{-2}$  is due to aerosol-radiation interactions, as also shown in  
226 Lund et al. (2018), and  $-0.42 \text{ W m}^{-2}$  due to aerosol-cloud interactions. Due to the rapid emission  
227 reductions projected over the next couple of decades, the RF is less than half in magnitude to its  
228 present-day value in SSP1-1.9 already by 2030, continuing to weaken at a slower rate after. In  
229 2100 (relative to 1750), the RFtotal is  $-0.04 \text{ W m}^{-2}$  in SSP1-1.9 and  $-0.20 \text{ W m}^{-2}$  in SSP2-4.5. With  
230 emissions following SSP3-7.0, the temporal evolution of RF is nearly flat through the 21<sup>st</sup> century  
231 and is  $-0.51 \text{ W m}^{-2}$  in 2100, only 8% lower in magnitude than in 2015. Even with weak air pollution  
232 control (SSP3-7.0) end-of-the-century emissions are slightly lower than the present-day level.  
233 Hence, looking only at the period 2015-2100, we estimate a positive aerosol forcing in all three  
234 scenarios considered. The RFtotal in 2100 relative to 2015 is  $0.51 \text{ W m}^{-2}$ ,  $0.35 \text{ W m}^{-2}$  and  $0.04 \text{ W}$   
235  $\text{m}^{-2}$  in SSP1-1.9, SSP2-4.5 and SSP3-7.0, respectively. The estimates presented here do not account  
236 for the rapid adjustments (or semi-direct effects) associated with BC. Using data from several  
237 global models, Stjern et al. (2017) found that the rapid adjustments by clouds offset a significant  
238 fraction of the aerosols' positive RFari, reducing the net BC climate impact. In contrast, a recent  
239 study by Allen et al. (2019) found positive cloud rapid adjustment. The latter finding would imply

240 a much stronger non-cloud negative rapid adjustment than presented in Smith et al. (2018) and  
241 methodological differences hence clearly need to be better resolved in order to understand the  
242 contrasting results.

243 Few modeling-based estimates for comparison with our results exist so far. In a recent study,  
244 Fiedler et al. (2019b) used a simple plume parameterization of optical properties and cloud effects  
245 of anthropogenic aerosols and scaled the present-day aerosol optical depth by the SSP emissions  
246 to derive estimates of future forcing. An effective radiative forcing (ERF) (comparable to our  
247 RF<sub>total</sub>) in the mid-2090s relative to 1850 ranging from  $-0.15 \text{ W m}^{-2}$  for SSP1-1.9 to  $-0.54 \text{ W m}^{-2}$   
248 for SSP3-7.0 was calculated. This is in reasonable agreement with the estimates derived in the  
249 present analysis, although we find a weaker forcing in SSP1-1.9. Using two idealized scenarios to  
250 span a broader range of emissions than represented in the RCPs, Partanen et al. (2018) also  
251 estimated a broad range in aerosol ERF, from  $-0.02 \text{ W m}^{-2}$  to  $-0.82 \text{ W m}^{-2}$ , in 2100 (relative to  
252 1850). The latter is significantly stronger than our SSP3-7.0 estimate. While not directly  
253 comparable due to differing emission inventories and methodologies, these studies reinforce our  
254 finding that weak air pollution control over the 21<sup>st</sup> century result in sustained strong negative  
255 aerosol forcing.

256 The spatiotemporal differences in trend documented above translates into effects on global and  
257 regional RF. In Fig. 4 we therefore show the change in RF<sub>total</sub> over four time periods, 1750-2015,  
258 1750-1990, 1990-2015 and 2015-2030 (for each SSP). Figure S3 show the corresponding results  
259 for RF<sub>ari</sub> and RF<sub>aci</sub> separately. Whereas the impact of anthropogenic aerosols is a negative RF<sub>total</sub>  
260 everywhere except over the high-albedo deserts and snow-covered regions when taken over the  
261 entire historical period 1750-2015, a positive RF is seen over North America, Europe and Russia  
262 after the 1990-2015 period, driven by decreased SO<sub>2</sub> emissions (and somewhat offset by a  
263 simultaneous decline in BC emissions). This positive RF is largely driven by aerosol-radiation  
264 interactions. Over South and East Asia, Africa and most of South America the RF<sub>total</sub> remains  
265 negative, although a significant fraction of the total impact since pre-industrial has already been  
266 realized before 1990. This weaker negative forcing is due to a combination of increasing BC  
267 emissions and a leveling off in SO<sub>2</sub> emissions in China in the CEDS inventory (Hosely et al. 2018).  
268 Globally, the combined effect is an increase in global-mean RF<sub>total</sub> over the 1990-2015 period of  
269  $+0.09 \text{ W m}^{-2}$ . Using the ECLIPSE emission inventory, Myhre et al. (2017) estimated an increase  
270 in the multi-model RF due to combined changes in aerosols and ozone from 1990 to 2015 of  $+0.17$   
271  $\text{W m}^{-2}$ , with about two-thirds of this from aerosols, i.e., similar to our results using the CEDS/SSP  
272 emissions.

273 Distinct regional differences are seen also during the period 2015-2030 under the different SSPs.  
274 With emissions following SSP1-1.9, we estimate a positive global-mean RF<sub>total</sub> of  $0.33 \text{ W m}^{-2}$ ,  
275 more than three times the RF<sub>total</sub> over the 1990-2015 period. In contrast to the 1900-2015 period,  
276 the strongest RF now comes from aerosol-cloud interactions, as emissions over continental  
277 northern hemisphere regions are low to begin with. The RF<sub>total</sub> is especially large over South and  
278 East Asia, and of opposite sign from what the region has experienced during the past decades.  
279 Smaller positive global mean RF<sub>total</sub> of  $0.08 \text{ W m}^{-2}$  is estimated also under SSP2-4.5 and SSP3-  
280 7.0 during this period. In contrast to SSP1-1.9, the RF remains negative over India under SSP2-  
281 4.5 and SSP3-7.0 where a continued increase in emissions of SO<sub>2</sub> is projected over the next decades.

282 In all SSPs, the  $RF_{total}$  over China switches from negative in the past decades to positive over the  
283 2015-2030 period. Recent studies suggest that Chinese  $SO_2$  emissions have declined even more  
284 than captured by the CEDS until 2014, indicating that this pattern of forcing may already have  
285 been partly realized (Li et al., 2017; Zheng et al., 2018). In contrast, emissions of India are  
286 projected to increase, at least initially. The potential implications of this feature are discussed in a  
287 separate paper (Samset et al., 2019). Weak RF is found over the African continent in the SSP2-4.5  
288 and SSP3-7.0 scenarios. However, as shown in Figure 2, aerosols will continue to affect local  
289 climate and air quality in this region.

290

#### 291 4 Discussion

292 Under a given scenario, emissions of all species generally follow the same global trend, although  
293 the rate of change differs between regions. However, over the recent years, emissions of  $SO_2$  have  
294 declined, whereas BC emissions have increased (Hoesly et al., 2018). Considering a hypothetical  
295 and simplified case where the mainly industrial, and perhaps easier to mitigate,  $SO_2$  emissions  
296 begin to decline rapidly also in other high emitting regions, whereas the mainly residential, more  
297 challenging, BC sources remain largely unchecked, the aerosol forcing may follow a different path  
298 than estimated here. As an illustrative example, we calculate the contribution to  $RF_{ari}$  in 2020 and  
299 2050 (relative to 1750) from individual components under SSP1-1.9 and SSP3-7.0 (Table S1).  
300 Taking the sum of the sulfate forcing from SSP1-1.9 and the remaining components from SSP3-  
301 7.0, the total  $RF_{ari}$  is  $-0.018 \text{ W m}^{-2}$  in 2020, i.e., significantly weaker than when all emissions  
302 follow SSP1-1.9, and  $0.15 \text{ W m}^{-2}$  in 2050. Continuing along the recent emission development of  
303 declining  $SO_2$  emissions and increasing BC could imply a different development in the total  
304 aerosol effect relative to pre-industrial than shown by the three scenarios here, at least towards the  
305 mid-century. We emphasize that these numbers are meant to be illustrative and note that significant  
306 uncertainties surround the climate impact of both BC and the co-emitted organic aerosols. As noted  
307 above, our estimates do not account for the rapid adjustments which might reduce the global  
308 surface temperature response to BC perturbations. Additionally, the role of absorption by so-called  
309 brown carbon remains an important uncertainty (Samset et al., 2018b). Previous work has also  
310 pointed to the possibility of substantial increases in radiative forcing by nitrate over the 21st  
311 century (Bauer et al., 2007; Bellouin et al., 2011; Shindell et al., 2013), and a notable increase in  
312 nitrate burden is also estimated in the present study when emissions follow SSP3-7.0. This  
313 translates into a nitrate RF that is almost a factor 2 stronger in 2100 than in 2020 and constitutes a  
314 correspondingly larger fraction of the  $RF_{total}$  in this scenario (Table S1)

315 We present projected future aerosol RF based on single-model simulations. Aerosols, however,  
316 remain one of the most uncertain drivers of climate change, with significant model spread resulting  
317 from several factors, including differences in the simulated aerosol distributions, optical properties  
318 and cloud fields. Myhre et al. (2013a) calculated a present-day aerosol  $RF_{ari}$  (relative to 1850)  
319 varying from  $-0.016 \text{ W m}^{-2}$  to  $-0.58 \text{ W m}^{-2}$  between 16 global models participating in the AeroCom  
320 Phase II experiment. Prescribing the distribution of anthropogenic aerosols, optical properties and  
321 effect on cloud droplet number concentration in six Earth System Models, Fiedler et al. (2019a)



322 find a model spread in aerosol ERF of  $-0.4 \text{ W m}^{-2}$  to  $-0.9 \text{ W m}^{-2}$ . Among the important  
323 consequences of high aerosol forcing uncertainty is the challenge it poses for estimating climate  
324 sensitivity. While in a scenario with declining aerosol emissions, combined with an increase in  
325 greenhouse gases, the uncertainty in the total anthropogenic forcing can be expected to decrease  
326 substantially even without scientific progress (Myhre et al., 2015), the high emission SSP3-7.0  
327 pathway suggest that aerosols may continue to be a confounding factor for constraining climate  
328 sensitivity.

329 While the scope of the present analysis is limited to radiative forcing, the calculated spread in end-  
330 of-century forcing under the SSPs will translate into a wide range of possible climate impacts. A  
331 number of studies have examined the future aerosol-induced radiative forcing and climate impacts  
332 using the RCP projections; see e.g., Westervelt et al. (2015) for a summary of papers published  
333 until 2013. While the magnitude of both present-day and future estimates differs between studies,  
334 the general characteristic is a significant weakening of the aerosol RF until 2100 in all scenarios.  
335 Other studies have investigated the potential for this rapid decline to drive near-term warming  
336 (Chalmers et al., 2012; Gillett & Von Salzen, 2013). However, while Chalmers et al. (2012) find  
337 a higher near-term warming in RCP2.6 than in RCP4.5 despite lower greenhouse gas forcing in  
338 the former, suggesting an important impact of falling aerosol emissions, Gillett and Von Salzen  
339 (2013) find no evidence that aerosol emissions reductions drive a particularly rapid near-term  
340 warming in this scenario. This points to the importance of inter-model differences in the response  
341 to aerosol perturbations. Under SSP1-1.9, aerosol emissions are projected to decline even more  
342 rapidly than in RCP2.6 over the coming couple of decades (Fig. 1). If in fact associated with a  
343 rapid warming, this development could further hinder the realization of the already ambitious  
344 temperature goals of the Paris agreement and this feature hence needs to be better quantified.  
345 Previous work also demonstrate effects of falling aerosol emissions also other climate variables  
346 such as mean and extreme precipitation (Navarro et al., 2017; Pendergrass et al., 2015) and  
347 atmospheric dynamics (Rotstayn et al., 2014). The numerous and significant impacts of aerosols  
348 underline the need to encompass the full range of projected emissions, regionally and globally, in  
349 future assessment, in particular in light of the crucial role of aerosols in shaping regional climate,  
350 regional assessments are needed to capture the impact of different trends.

351 It is well-established that future changes in aerosols will critically affect local air quality. Silva et  
352 al. (2016) found avoided premature mortality in 2100 of between  $-2.39$  and  $-1.31$  million deaths  
353 per year for the four RCP. Partanen et al. (2018) estimated almost 80% fewer PM<sub>2.5</sub>-induced  
354 deaths per year in 2100 under RCP4.5 compared to 2010. In contrast, an idealized high aerosol  
355 scenario resulted in 17% increase in premature mortality by 2030. These numbers where estimated  
356 using present-day population density. Under all SSPs, considerable increases in population density  
357 is projected in Africa, the Middle East and South Asia (Jones & O'Neill, 2016) – regions that are  
358 also identified as hotspots for exposure and vulnerability to multi-sector climate risk (Byers et al.,  
359 2018). In the present study, we estimate an increase in the average surface concentration of  
360 anthropogenic aerosols (i.e., BC, POA, sulfate and fine mode nitrate) of 17% and 25% by 2100

361 under SSP3-7.0 in South Asia and North Africa plus the Middle East, respectively. Air pollution  
362 issues are not limited to developing countries. While all scenarios project reductions in surface  
363 aerosol concentrations in Europe, North America and Russia, there are substantial differences in  
364 the magnitude, from 35-20% lower by 2100 in SSP3-7.0 to around 70% lower in SSP1-1.9,  
365 highlighting the potential for further air quality improvements globally.

366 Our estimates of RF<sub>aci</sub> exclude contributions from cloud lifetime changes. The estimates of cloud  
367 lifetime effect are generally lower in recent studies than in early work, but still give non-negligible  
368 contribution to the aerosol forcing (Storelvmo, 2017). Our study does not account for potential  
369 impacts of climate change on circulation, precipitation or chemistry, which can affect the lifetime  
370 and transport pathways, as well as emissions, of the aerosols. For instance, Bellouin et al. (2011)  
371 found increasing atmospheric residence times over the 21<sup>st</sup> century as wet deposition rates  
372 decreased. Including both changing climate and emissions, Pommier et al. (2018) suggested that  
373 concentrations of particulate matter (PM<sub>2.5</sub>) will increase by up to 6.5% over the Indo-Gangetic  
374 Plain to 2050, driven by increases in dust, particulate organic matter and secondary inorganic  
375 aerosols through changes in precipitation, biogenic emissions and wind speed. Hence, by keeping  
376 natural sources of emissions fixed at present-day levels, our results may underestimate the future  
377 aerosols loads. Moreover, a recent review of climate feedbacks on aerosol distributions suggests  
378 that in regions where anthropogenic aerosol loadings decrease, the impacts of climate on the  
379 variability of natural aerosols increase (Tegen & Schepanski, 2018). Changing climatic conditions  
380 may also affect the radiative forcing through changing cloud distributions and surface albedo.  
381 While our approach clearly disentangles and assesses the changes in aerosols resulting from  
382 changes in anthropogenic emissions, representation and knowledge of feedback processes are  
383 important for understanding the full role of future aerosols in the climate system.

384

## 385 5 Conclusions

386 Using a global chemistry transport model and radiative transfer modeling, we have estimated the  
387 projected future loading and radiative forcing of anthropogenic aerosols under the most recent  
388 generation of scenarios, the Shared Socioeconomic Pathways. These new air pollution scenarios  
389 link varying degrees of air pollution control to the socioeconomic narratives underlying the SSPs  
390 and climate forcing targets, spanning a much broader range of plausible future emission  
391 trajectories than previous scenarios. Here we have used three scenarios: SSP3-7.0 (weak air  
392 pollution control, high mitigation and adaptation challenges), SSP2-4.5 (medium pollution control,  
393 medium mitigation and adaptation challenges) and SSP1-1.9 (strong pollution control, low  
394 mitigation and adaptation challenges). In all three scenarios, we estimate a positive aerosol forcing  
395 over the period 2015-2100, although with very different timing and magnitude depending on  
396 stringency of air pollution control. The end-of-century aerosol forcing relative to 2015 is 0.51 W  
397 m<sup>-2</sup> with emissions following SSP1-1.9, 0.35 W m<sup>-2</sup> in SSP2-4.5 and 0.04 W m<sup>-2</sup> in SSP3-7.0.  
398 While effective air pollution control and socioeconomic development following SSP1-1.9 results  
399 in a rapid weakening of the aerosol RF compared to the pre-industrial to present-day level already  
400 by 2030, there is little change in the global mean aerosol forcing over the 21<sup>st</sup> century in a

401 regionally fragmented world with slower mitigation progress (SSP3-7.0). Significant  
402 spatiotemporal differences in trends are also highlighted. Most notably, under weak air pollution  
403 control, aerosol loadings in East and South Asia temporarily increase from present levels but start  
404 to decline after 2050 and return to current levels of slightly below by 2100. North Africa and the  
405 Middle East reaches the levels of South Asia by the end of the century and there is no declining  
406 trend this century. The present analysis is limited to the documentation of radiative forcing and  
407 aerosol loads. Under both rapidly declining and sustained high emissions, aerosols will play an  
408 important role in shaping and affect regional and global climate.

409

#### 410 Code availability

411 Oslo CTM3 is stored in a SVN repository at the University of Oslo central subversion system  
412 and is available upon request. Please contact [m.t.lund@cicero.oslo.no](mailto:m.t.lund@cicero.oslo.no). In this paper, we use the  
413 official version 1.0, Oslo CTM3 v1.0.

414

#### 415 Data availability

416 The gridded SSP anthropogenic emission data are published within the ESGF system [https://esgf-](https://esgf-node.llnl.gov/search/input4mips/)  
417 [node.llnl.gov/search/input4mips/](https://esgf-node.llnl.gov/search/input4mips/) (last access: December 2018). Model output and post-processing  
418 routines are available upon request from Marianne T. Lund ([m.t.lund@cicero.oslo.no](mailto:m.t.lund@cicero.oslo.no)).

419

#### 420 Author contributions

421 MTL performed the Oslo CTM3 experiments and led the analysis and writing. GM performed the  
422 radiative transfer modeling and BHS contributed with graphics production. All authors contributed  
423 during the writing of the paper.

424

425

#### 426 Acknowledgements

427 The authors acknowledge funding from the Norwegian Research Council through grants 248834  
428 (QUISARC) and 240372 (AC/BC). We also acknowledge the Research Council of Norway's  
429 programme for supercomputing (NOTUR).

430

#### 431 Competing interests

432 The authors declare that they have no conflict of interest.

433

434

#### 435 References

436 Allen R. J., Amiri-Farahani A., Lamarque J.-F., Smith C., Shindell D., Hassan T. &  
437 Chung C. E.: Observationally constrained aerosol–cloud semi-direct effects, *npj Climate and*  
438 *Atmospheric Science*. 2(1), 16, 10.1038/s41612-019-0073-9, 2019.

439 Amann M., Klimont Z. & Wagner F.: Regional and Global Emissions of Air Pollutants:  
440 Recent Trends and Future Scenarios, *Annual Review of Environment and Resources*. 38(1), 31-  
441 55, 10.1146/annurev-environ-052912-173303, 2013.

442 Balakrishnan K., Dey S., Gupta T., Dhaliwal R. S., Brauer M., Cohen A. J., Stanaway J.  
443 D., Beig G., Joshi T. K., Aggarwal A. N., Sabde Y., Sadhu H., Frostad J., Causey K., Godwin  
444 W., Shukla D. K., Kumar G. A., Varghese C. M., Muraleedharan P., Agrawal A., Anjana R. M.,  
445 Bhansali A., Bhardwaj D., Burkart K., Cercy K., Chakma J. K., Chowdhury S., Christopher D.  
446 J., Dutta E., Furtado M., Ghosh S., Ghoshal A. G., Glenn S. D., Guleria R., Gupta R., Jeemon P.,  
447 Kant R., Kant S., Kaur T., Koul P. A., Krish V., Krishna B., Larson S. L., Madhipatla K.,  
448 Mahesh P. A., Mohan V., Mukhopadhyay S., Mutreja P., Naik N., Nair S., Nguyen G., Odell C.  
449 M., Pandian J. D., Prabhakaran D., Prabhakaran P., Roy A., Salvi S., Sambandam S., Saraf D.,  
450 Sharma M., Shrivastava A., Singh V., Tandon N., Thomas N. J., Torre A., Xavier D., Yadav G.,  
451 Singh S., Shekhar C., Vos T., Dandona R., Reddy K. S., Lim S. S., Murray C. J. L., Venkatesh S.  
452 & Dandona L.: The impact of air pollution on deaths, disease burden, and life expectancy across  
453 the states of India: the Global Burden of Disease Study 2017, *The Lancet Planetary Health*. 3(1),  
454 e26-e39, [https://doi.org/10.1016/S2542-5196\(18\)30261-4](https://doi.org/10.1016/S2542-5196(18)30261-4), 2019.

455 Bauer S. E., Koch D., Unger N., Metzger S. M., Shindell D. T. & Streets D. G.: Nitrate  
456 aerosols today and in 2030: a global simulation including aerosols and tropospheric ozone,  
457 *Atmospheric Chemistry and Physics*. 7(19), 5043-5059, 2007.

458 Bellouin N., Rae J., Jones A., Johnson C., Haywood J. & Boucher O.: Aerosol forcing in  
459 the Climate Model Intercomparison Project (CMIP5) simulations by HadGEM2-ES and the role  
460 of ammonium nitrate, *Journal of Geophysical Research-Atmospheres*. 116, D20206,  
461 10.1029/2011jd016074, 2011.

462 Bian H., Chin M., Hauglustaine D. A., Schulz M., Myhre G., Bauer S. E., Lund M. T.,  
463 Karydis V. A., Kucsera T. L., Pan X., Pozzer A., Skeie R. B., Steenrod S. D., Sudo K., Tsigaridis  
464 K., Tsimpidi A. P. & Tsyro S. G.: Investigation of global particulate nitrate from the AeroCom  
465 Phase III experiment, *Atmos. Chem. Phys.* 2017(17), 12911-12940, <https://doi.org/10.5194/acp-17-12911-2017>, 2017.

467 Byers E., Gidden M., Leclère D., Balkovic J., Burek P., Ebi K., Greve P., Grey D.,  
468 Havlik P., Hillers A., Johnson N., Kahil T., Krey V., Langan S., Nakicenovic N., Novak R.,  
469 Obersteiner M., Pachauri S., Palazzo A., Parkinson S., Rao N. D., Rogelj J., Satoh Y., Wada Y.,  
470 Willaarts B. & Riahi K.: Global exposure and vulnerability to multi-sector development and  
471 climate change hotspots, *Environmental Research Letters*. 13(5), 055012, 10.1088/1748-  
472 9326/aabf45, 2018.

473 Chalmers N., Highwood E. J., Hawkins E., Sutton R. & Wilcox L. J.: Aerosol  
474 contribution to the rapid warming of near-term climate under RCP 2.6, *Geophysical Research*  
475 *Letters*. 39(18), doi:10.1029/2012GL052848, 2012.

476 Chuwah C., van Noije T., van Vuuren D. P., Hazeleger W., Strunk A., Deetman S.,  
477 Beltran A. M. & van Vliet J.: Implications of alternative assumptions regarding future air  
478 pollution control in scenarios similar to the Representative Concentration Pathways,  
479 *Atmospheric Environment*. 79, 787-801, <https://doi.org/10.1016/j.atmosenv.2013.07.008>, 2013.

480 Fiedler S., Kinne S., Huang W. T. K., Räisänen P., O'Donnell D., Bellouin N., Stier P.,  
481 Merikanto J., van Noije T., Makkonen R. & Lohmann U.: Anthropogenic aerosol forcing –  
482 insights from multiple estimates from aerosol-climate models with reduced complexity, *Atmos.*  
483 *Chem. Phys.* 19(10), 6821-6841, 10.5194/acp-19-6821-2019, 2019a.

484 Fiedler S., Stevens B., Gidden M., Smith S. J., Riahi K. & van Vuuren D.: First forcing  
485 estimates from the future CMIP6 scenarios of anthropogenic aerosol optical properties and an  
486 associated Twomey effect, *Geosci. Model Dev.* 12(3), 989-1007, 10.5194/gmd-12-989-2019,  
487 2019b.

488 Fricko O., Havlik P., Rogelj J., Klimont Z., Gusti M., Johnson N., Kolp P., Strubegger  
489 M., Valin H., Amann M., Ermolieva T., Forsell N., Herrero M., Heyes C., Kindermann G., Krey  
490 V., McCollum D. L., Obersteiner M., Pachauri S., Rao S., Schmid E., Schoepp W. & Riahi K.:  
491 The marker quantification of the Shared Socioeconomic Pathway 2: A middle-of-the-road  
492 scenario for the 21st century, *Global Environmental Change.* 42, 251-267,  
493 <https://doi.org/10.1016/j.gloenvcha.2016.06.004>, 2017.

494 Fujimori S., Hasegawa T., Masui T., Takahashi K., Herran D. S., Dai H., Hijioka Y. &  
495 Kainuma M.: SSP3: AIM implementation of Shared Socioeconomic Pathways, *Global  
496 Environmental Change.* 42, 268-283, <https://doi.org/10.1016/j.gloenvcha.2016.06.009>, 2017.

497 Gidden M. J., Riahi K., Smith S. J., Fujimori S., Luderer G., Kriegler E., van Vuuren D.  
498 P., van den Berg M., Feng L., Klein D., Calvin K., Doelman J. C., Frank S., Fricko O., Harmsen  
499 M., Hasegawa T., Havlik P., Hilaire J., Hoesly R., Horing J., Popp A., Stehfest E. & Takahashi  
500 K.: Global emissions pathways under different socioeconomic scenarios for use in CMIP6: a  
501 dataset of harmonized emissions trajectories through the end of the century, *Geosci. Model Dev.*  
502 12(4), 1443-1475, 10.5194/gmd-12-1443-2019, 2019.

503 Gillett N. P. & Von Salzen K.: The role of reduced aerosol precursor emissions in driving  
504 near-term warming, *Environmental Research Letters.* 8(3), 034008, 10.1088/1748-  
505 9326/8/3/034008, 2013.

506 Granier C., Bessagnet B., Bond T., D'Angiola A., Denier van der Gon H., Frost G. J.,  
507 Heil A., Kaiser J. W., Kinne S., Klimont Z., Kloster S., Lamarque J.-F., Liousse C., Masui T.,  
508 Meleux F., Mieville A., Ohara T., Raut J.-C., Riahi K., Schultz M. G., Smith S. J., Thompson A.,  
509 van Aardenne J., van der Werf G. R. & van Vuuren D. P.: Evolution of anthropogenic and  
510 biomass burning emissions of air pollutants at global and regional scales during the 1980–2010  
511 period, *Climatic Change.* 109(1), 163, 10.1007/s10584-011-0154-1, 2011.

512 Hoesly R. M., Smith S. J., Feng L., Klimont Z., Janssens-Maenhout G., Pitkanen T.,  
513 Seibert J. J., Vu L., Andres R. J., Bolt R. M., Bond T. C., Dawidowski L., Kholod N., Kurokawa  
514 J. I., Li M., Liu L., Lu Z., Moura M. C. P., O'Rourke P. R. & Zhang Q.: Historical (1750–2014)  
515 anthropogenic emissions of reactive gases and aerosols from the Community Emission Data  
516 System (CEDS), *Geosci. Model Dev.* 2018(11), 369-408, [https://doi.org/10.5194/gmd-11-369-  
517 2018](https://doi.org/10.5194/gmd-11-369-2018), 2018.

518 IPCC: Summary for Policymakers. In: *Global warming of 1.5°C. An IPCC Special  
519 Report on the impacts of global warming of 1.5°C above pre-industrial levels and related global  
520 greenhouse gas emission pathways, in the context of strengthening the global response to the  
521 threat of climate change, sustainable development, and efforts to eradicate poverty* [V. Masson-  
522 Delmotte, P. Zhai, H. O. Pörtner, D. Roberts, J. Skea, P. R. Shukla, A. Pirani, W. Moufouma-  
523 Okia, C. Péan, R. Pidcock, S. Connors, J. B. R. Matthews, Y. Chen, X. Zhou, M. I. Gomis, E.  
524 Lonnoy, T. Maycock, M. Tignor, T. Waterfield (eds.)]. World Meteorological Organization,  
525 Geneva, Switzerland, 32 pp., 2018.

526 Jones B. & O'Neill B. C.: Spatially explicit global population scenarios consistent with  
527 the Shared Socioeconomic Pathways, *Environmental Research Letters.* 11(8), 084003,  
528 10.1088/1748-9326/11/8/084003, 2016.

529 Li C., McLinden C., Fioletov V., Krotkov N., Carn S., Joiner J., Streets D., He H., Ren  
530 X., Li Z. & Dickerson R. R.: India Is Overtaking China as the World's Largest Emitter of  
531 Anthropogenic Sulfur Dioxide, *Scientific Reports*. 7(1), 14304, 10.1038/s41598-017-14639-8,  
532 2017.

533 Li K., Liao H., Zhu J. & Moch J. M.: Implications of RCP emissions on future PM<sub>2.5</sub> air  
534 quality and direct radiative forcing over China, *Journal of Geophysical Research: Atmospheres*.  
535 121(21), 12,985-913,008, doi:10.1002/2016JD025623, 2016.

536 Liang C. K., West J. J., Silva R. A., Bian H., Chin M., Davila Y., Dentener F. J., Emmons  
537 L., Flemming J., Folberth G., Henze D., Im U., Jonson J. E., Keating T. J., Kucsera T., Lenzen  
538 A., Lin M., Lund M. T., Pan X., Park R. J., Pierce R. B., Sekiya T., Sudo K. & Takemura T.:  
539 HTAP2 multi-model estimates of premature human mortality due to intercontinental transport of  
540 air pollution and emission sectors, *Atmos. Chem. Phys.* 18(14), 10497-10520, 10.5194/acp-18-  
541 10497-2018, 2018.

542 Lund M. T., Myhre G., Haslerud A. S., Skeie R. B., Griesfeller J., Platt S. M., Kumar R.,  
543 Myhre C. L. & Schulz M.: Concentrations and radiative forcing of anthropogenic aerosols from  
544 1750 to 2014 simulated with the Oslo CTM3 and CEDS emission inventory, *Geosci. Model Dev.*  
545 11(12), 4909-4931, 10.5194/gmd-11-4909-2018, 2018.

546 Myhre G., Samset B. H., Schulz M., Balkanski Y., Bauer S., Bernsten T. K., Bian H.,  
547 Bellouin N., Chin M., Diehl T., Easter R. C., Feichter J., Ghan S. J., Hauglustaine D., Iversen T.,  
548 Kinne S., Kirkevåg A., Lamarque J. F., Lin G., Liu X., Lund M. T., Luo G., Ma X., van Noije T.,  
549 Penner J. E., Rasch P. J., Ruiz A., Seland Ø., Skeie R. B., Stier P., Takemura T., Tsigaridis K.,  
550 Wang P., Wang Z., Xu L., Yu H., Yu F., Yoon J. H., Zhang K., Zhang H. & Zhou C.: Radiative  
551 forcing of the direct aerosol effect from AeroCom Phase II simulations, *Atmos. Chem. Phys.*  
552 13(4), 1853-1877, 10.5194/acp-13-1853-2013, 2013a.

553 Myhre G., Shindell D., Brèon F.-M., Collins W., Fuglestedt J., Huang J., Koch D.,  
554 Lamarque J.-F., Lee D., Mendoza B., Nakajima T., Robock A., Stephens G., Takemura T. &  
555 Zhang H.: Anthropogenic and natural radiative forcing. In: *Climate Change 2013: The Physical  
556 Science Basis. Contribution of Working Group I to the Fifth Assessment Report of the  
557 Intergovernmental Panel on Climate Change* [Stocker, T.F., D., Qin, G.-K. Plattner, M. Tignor,  
558 S.K. Allen, J. Boschung, A. Nauels, Y. Xia, V. Bex and P.M. Midgley (eds). Cambridge  
559 University Press, Cambridge, United Kingdom and New York, NY, USA 2013b.

560 Myhre G., Boucher O., Brèon F.-M., Forster P. & Shindell D.: Declining uncertainty in  
561 transient climate response as CO<sub>2</sub> forcing dominates future climate change, *Nature Geoscience*.  
562 8, 181, 10.1038/ngeo2371

563 <https://www.nature.com/articles/ngeo2371#supplementary-information>, 2015.

564 Myhre G., Aas W., Cherian R., Collins W., Faluvegi G., Flanner M., Forster P.,  
565 Hodnebrog Ø., Klimont Z., Lund M. T., Mülmenstädt J., Lund Myhre C., Olivé D., Prather M.,  
566 Quaas J., Samset B. H., Schnell J. L., Schulz M., Shindell D., Skeie R. B., Takemura T. & Tsyro  
567 S.: Multi-model simulations of aerosol and ozone radiative forcing due to anthropogenic  
568 emission changes during the period 1990–2015, *Atmos. Chem. Phys.* 17(4), 2709-2720,  
569 10.5194/acp-17-2709-2017, 2017.

570 Navarro J. C. A., Ekman A. M. L., Pausata F. S. R., Lewinschal A., Varma V., Seland Ø.,  
571 Gauss M., Iversen T., Kirkevåg A., Riipinen I. & Hansson H. C.: Future Response of  
572 Temperature and Precipitation to Reduced Aerosol Emissions as Compared with Increased  
573 Greenhouse Gas Concentrations, *Journal of Climate*. 30(3), 939-954, 10.1175/jcli-d-16-0466.1,  
574 2017.

575 Nazarenko L., Schmidt G. A., Miller R. L., Tausnev N., Kelley M., Ruedy R., Russell G.  
576 L., Aleinov I., Bauer M., Bauer S., Bleck R., Canuto V., Cheng Y., Clune T. L., Del Genio A.  
577 D., Faluvegi G., Hansen J. E., Healy R. J., Kiang N. Y., Koch D., Lacis A. A., LeGrande A. N.,  
578 Lerner J., Lo K. K., Menon S., Oinas V., Perlwitz J., Puma M. J., Rind D., Romanou A., Sato  
579 M., Shindell D. T., Sun S., Tsigaridis K., Unger N., Voulgarakis A., Yao M.-S. & Zhang J.:  
580 Future climate change under RCP emission scenarios with GISS ModelE2, *Journal of Advances*  
581 *in Modeling Earth Systems*. 7(1), 244-267, doi:10.1002/2014MS000403, 2015.

582 O'Neill B. C., Kriegler E., Riahi K., Ebi K. L., Hallegatte S., Carter T. R., Mathur R. &  
583 van Vuuren D. P.: A new scenario framework for climate change research: the concept of shared  
584 socioeconomic pathways, *Climatic Change*. 122(3), 387-400, 10.1007/s10584-013-0905-2, 2014.

585 Ocko I. B., Ramaswamy V. & Ming Y.: Contrasting Climate Responses to the Scattering  
586 and Absorbing Features of Anthropogenic Aerosol Forcings, *Journal of Climate*. 27(14), 5329-  
587 5345, 10.1175/jcli-d-13-00401.1, 2014.

588 Partanen A.-I., Landry J.-S. & Matthews H. D.: Climate and health implications of future  
589 aerosol emission scenarios, *Environmental Research Letters*. 13(2), 024028, 10.1088/1748-  
590 9326/aaa511, 2018.

591 Pendergrass A. G., Lehner F., Sanderson B. M. & Xu Y.: Does extreme precipitation  
592 intensity depend on the emissions scenario?, *Geophysical Research Letters*. 42(20), 8767-8774,  
593 doi:10.1002/2015GL065854, 2015.

594 Pommier M., Fagerli H., Gauss M., Simpson D., Sharma S., Sinha V., Ghude S. D.,  
595 Landgren O., Nyiri A. & Wind P.: Impact of regional climate change and future emission  
596 scenarios on surface O<sub>3</sub> and PM<sub>2.5</sub> over India, *Atmos. Chem. Phys.* 18(1), 103-127,  
597 10.5194/acp-18-103-2018, 2018.

598 Quaas J., Boucher O. & Lohmann U.: Constraining the total aerosol indirect effect in the  
599 LMDZ and ECHAM4 GCMs using MODIS satellite data, *Atmos. Chem. Phys.* 6(4), 947-955,  
600 10.5194/acp-6-947-2006, 2006.

601 Rao S., Pachauri S., Dentener F., Kinney P., Klimont Z., Riahi K. & Schoepp W.: Better  
602 air for better health: Forging synergies in policies for energy access, climate change and air  
603 pollution, *Global Environmental Change*. 23(5), 1122-1130,  
604 <https://doi.org/10.1016/j.gloenvcha.2013.05.003>, 2013.

605 Rao S., Klimont Z., Smith S. J., Van Dingenen R., Dentener F., Bouwman L., Riahi K.,  
606 Amann M., Bodirsky B. L., van Vuuren D. P., Aleluia Reis L., Calvin K., Drouet L., Fricko O.,  
607 Fujimori S., Gernaat D., Havlik P., Harmsen M., Hasegawa T., Heyes C., Hilaire J., Luderer G.,  
608 Masui T., Stehfest E., Strefler J., van der Sluis S. & Tavoni M.: Future air pollution in the Shared  
609 Socio-economic Pathways, *Global Environmental Change*. 42, 346-358,  
610 <https://doi.org/10.1016/j.gloenvcha.2016.05.012>, 2017.

611 Riahi K., Grübler A. & Nakicenovic N.: Scenarios of long-term socio-economic and  
612 environmental development under climate stabilization, *Technological Forecasting and Social*  
613 *Change*. 74(7), 887-935, <https://doi.org/10.1016/j.techfore.2006.05.026>, 2007.

614 Rogelj J., Rao S., McCollum D. L., Pachauri S., Klimont Z., Krey V. & Riahi K.: Air-  
615 pollution emission ranges consistent with the representative concentration pathways, *Nature*  
616 *Climate Change*. 4, 446, 10.1038/nclimate2178  
617 <https://www.nature.com/articles/nclimate2178#supplementary-information>, 2014.

618 Rotstayn L. D., Plymin E. L., Collier M. A., Boucher O., Dufresne J.-L., Luo J.-J., Salzen  
619 K. v., Jeffrey S. J., Foujols M.-A., Ming Y. & Horowitz L. W.: Declining Aerosols in CMIP5

620 Projections: Effects on Atmospheric Temperature Structure and Midlatitude Jets, *Journal of*  
621 *Climate*. 27(18), 6960-6977, 10.1175/jcli-d-14-00258.1, 2014.

622 Ru M., Shindell D. T., Seltzer K. M., Tao S. & Zhong Q.: The long-term relationship  
623 between emissions and economic growth for SO<sub>2</sub>, CO<sub>2</sub>, and BC, *Environmental Research*  
624 *Letters*. 13(12), 124021, 10.1088/1748-9326/aaece2, 2018.

625 Samset B. H., Myhre G., Forster P. M., Hodnebrog Ø., Andrews T., Faluvegi G.,  
626 Fläschner D., Kasoar M., Kharin V., Kirkevåg A., Lamarque J.-F., Olivié D., Richardson T.,  
627 Shindell D., Shine K. P., Takemura T. & Voulgarakis A.: Fast and slow precipitation responses  
628 to individual climate forcings: A PDRMIP multimodel study, *Geophysical Research Letters*.  
629 43(6), 2782-2791, 10.1002/2016gl068064, 2016.

630 Samset B. H.: How cleaner air changes the climate, *Science*. 360(6385), 148-150,  
631 10.1126/science.aat1723, 2018.

632 Samset B. H., Sand M., Smith C. J., Bauer S. E., Forster P. M., Fuglestedt J. S., Osprey  
633 S. & Schleussner C.-F.: Climate Impacts From a Removal of Anthropogenic Aerosol Emissions,  
634 *Geophysical Research Letters*. 45(2), 1020-1029, doi:10.1002/2017GL076079, 2018a.

635 Samset B. H., Stjern C. W., Andrews E., Kahn R. A., Myhre G., Schulz M. & Schuster G.  
636 L.: Aerosol Absorption: Progress Towards Global and Regional Constraints, *Current Climate*  
637 *Change Reports*, 10.1007/s40641-018-0091-4, 2018b.

638 Samset B. H., Lund M. T., Bollasina M., Wilcox L. & Myhre G.: Rapidly emerging  
639 patterns of Asian aerosol forcing, *Nature Geoscience* 12, 582-584, 2019.

640 Shindell D. T., Lamarque J. F., Schulz M., Flanner M., Jiao C., Chin M., Young P. J., Lee  
641 Y. H., Rotstayn L., Mahowald N., Milly G., Faluvegi G., Balkanski Y., Collins W. J., Conley A.  
642 J., Dalsoren S., Easter R., Ghan S., Horowitz L., Liu X., Myhre G., Nagashima T., Naik V.,  
643 Rumbold S. T., Skeie R., Sudo K., Szopa S., Takemura T., Voulgarakis A., Yoon J. H. & Lo F.:  
644 Radiative forcing in the ACCMIP historical and future climate simulations, *Atmos. Chem. Phys.*  
645 13(6), 2939-2974, 10.5194/acp-13-2939-2013, 2013.

646 Silva R. A., West J. J., Lamarque J. F., Shindell D. T., Collins W. J., Dalsoren S.,  
647 Faluvegi G., Folberth G., Horowitz L. W., Nagashima T., Naik V., Rumbold S. T., Sudo K.,  
648 Takemura T., Bergmann D., Cameron-Smith P., Cionni I., Doherty R. M., Eyring V., Josse B.,  
649 MacKenzie I. A., Plummer D., Righi M., Stevenson D. S., Strode S., Szopa S. & Zengast G.: The  
650 effect of future ambient air pollution on human premature mortality to 2100 using output from  
651 the ACCMIP model ensemble, *Atmos. Chem. Phys.* 16(15), 9847-9862, 10.5194/acp-16-9847-  
652 2016, 2016.

653 Smith C. J., Kramer R. J., Myhre G., Forster P. M., Soden B. J., Andrews T., Boucher O.,  
654 Faluvegi G., Fläschner D., Hodnebrog Ø., Kasoar M., Kharin V., Kirkevåg A., Lamarque J.-F.,  
655 Mülmenstädt J., Olivié D., Richardson T., Samset B. H., Shindell D., Stier P., Takemura T.,  
656 Voulgarakis A. & Watson-Parris D.: Understanding Rapid Adjustments to Diverse Forcing  
657 Agents, *Geophysical Research Letters*. 45(21), 12,023-012,031, 10.1029/2018gl079826, 2018.

658 Smith S. J. & Wigley T. M. L.: Multi-Gas Forcing Stabilization with Minicam, *The*  
659 *Energy Journal*. 27, 373-391, 2006.

660 Stamnes K., Tsay S. C., Wiscombe W. & Jayaweera K.: Numerically stable algorithm for  
661 discrete-ordinate-method radiative transfer in multiple scattering and emitting layered media,  
662 *Appl. Opt.* 27(12), 2502-2509, 10.1364/AO.27.002502, 1988.

663 Stjern C. W., Samset B. H., Myhre G., Bian H., Chin M., Davila Y., Dentener F.,  
664 Emmons L., Flemming J., Haslerud A. S., Henze D., Jonson J. E., Kucsera T., Lund M. T.,  
665 Schulz M., Sudo K., Takemura T. & Tilmes S.: Global and regional radiative forcing from 20 %



666 reductions in BC, OC and SO<sub>4</sub> – an HTAP2 multi-model study, *Atmos. Chem. Phys.* 16(21),  
667 13579-13599, 10.5194/acp-16-13579-2016, 2016.

668 Stjern C. W., Samset B. H., Myhre G., Forster P. M., Hodnebrog Ø., Andrews T.,  
669 Boucher O., Faluvegi G., Iversen T., Kasoar M., Kharin V., Kirkevåg A., Lamarque J.-F., Olivie  
670 D., Richardson T., Shawki D., Shindell D., Smith C. J., Takemura T. & Voulgarakis A.: Rapid  
671 Adjustments Cause Weak Surface Temperature Response to Increased Black Carbon  
672 Concentrations, *Journal of Geophysical Research: Atmospheres.* 122(21), 11,462-411,481,  
673 10.1002/2017JD027326, 2017.

674 Storelvmo T.: Aerosol Effects on Climate via Mixed-Phase and Ice Clouds, *Annual*  
675 *Review of Earth and Planetary Sciences.* 45(1), 199-222, 10.1146/annurev-earth-060115-  
676 012240, 2017.

677 Szopa S., Balkanski Y., Schulz M., Bekki S., Cugnet D., Fortems-Cheiney A., Turquety  
678 S., Cozic A., Déandréis C., Hauglustaine D., Idelkadi A., Lathière J., Lefevre F., Marchand M.,  
679 Vuolo R., Yan N. & Dufresne J.-L.: Aerosol and ozone changes as forcing for climate evolution  
680 between 1850 and 2100, *Climate Dynamics.* 40(9), 2223-2250, 10.1007/s00382-012-1408-y,  
681 2013.

682 Søvde O. A., Prather M. J., Isaksen I. S. A., Berntsen T. K., Stordal F., Zhu X., Holmes  
683 C. D. & Hsu J.: The chemical transport model Oslo CTM3, *Geosci. Model Dev.* 5(6), 1441-  
684 1469, 10.5194/gmd-5-1441-2012, 2012.

685 Tan J., Fu J. S., Dentener F., Sun J., Emmons L., Tilmes S., Flemming J., Takemura T.,  
686 Bian H., Zhu Q., Yang C. E. & Keating T.: Source contributions to sulfur and nitrogen  
687 deposition – an HTAP II multi-model study on hemispheric transport, *Atmos. Chem. Phys.*  
688 18(16), 12223-12240, 10.5194/acp-18-12223-2018, 2018.

689 Tegen I. & Schepanski K.: Climate Feedback on Aerosol Emission and Atmospheric  
690 Concentrations, *Current Climate Change Reports.* 4(1), 1-10, 10.1007/s40641-018-0086-1, 2018.

691 van Vuuren D. P., den Elzen M. G. J., Lucas P. L., Eickhout B., Strengers B. J., van  
692 Ruijven B., Wonink S. & van Houdt R.: Stabilizing greenhouse gas concentrations at low levels:  
693 an assessment of reduction strategies and costs, *Climatic Change.* 81(2), 119-159,  
694 10.1007/s10584-006-9172-9, 2007.

695 van Vuuren D. P., Stehfest E., Gernaat D. E. H. J., Doelman J. C., van den Berg M.,  
696 Harmsen M., de Boer H. S., Bouwman L. F., Daioglou V., Edelenbosch O. Y., Girod B., Kram  
697 T., Lassaletta L., Lucas P. L., van Meijl H., Müller C., van Ruijven B. J., van der Sluis S. &  
698 Tabeau A.: Energy, land-use and greenhouse gas emissions trajectories under a green growth  
699 paradigm, *Global Environmental Change.* 42, 237-250,  
700 <https://doi.org/10.1016/j.gloenvcha.2016.05.008>, 2017.

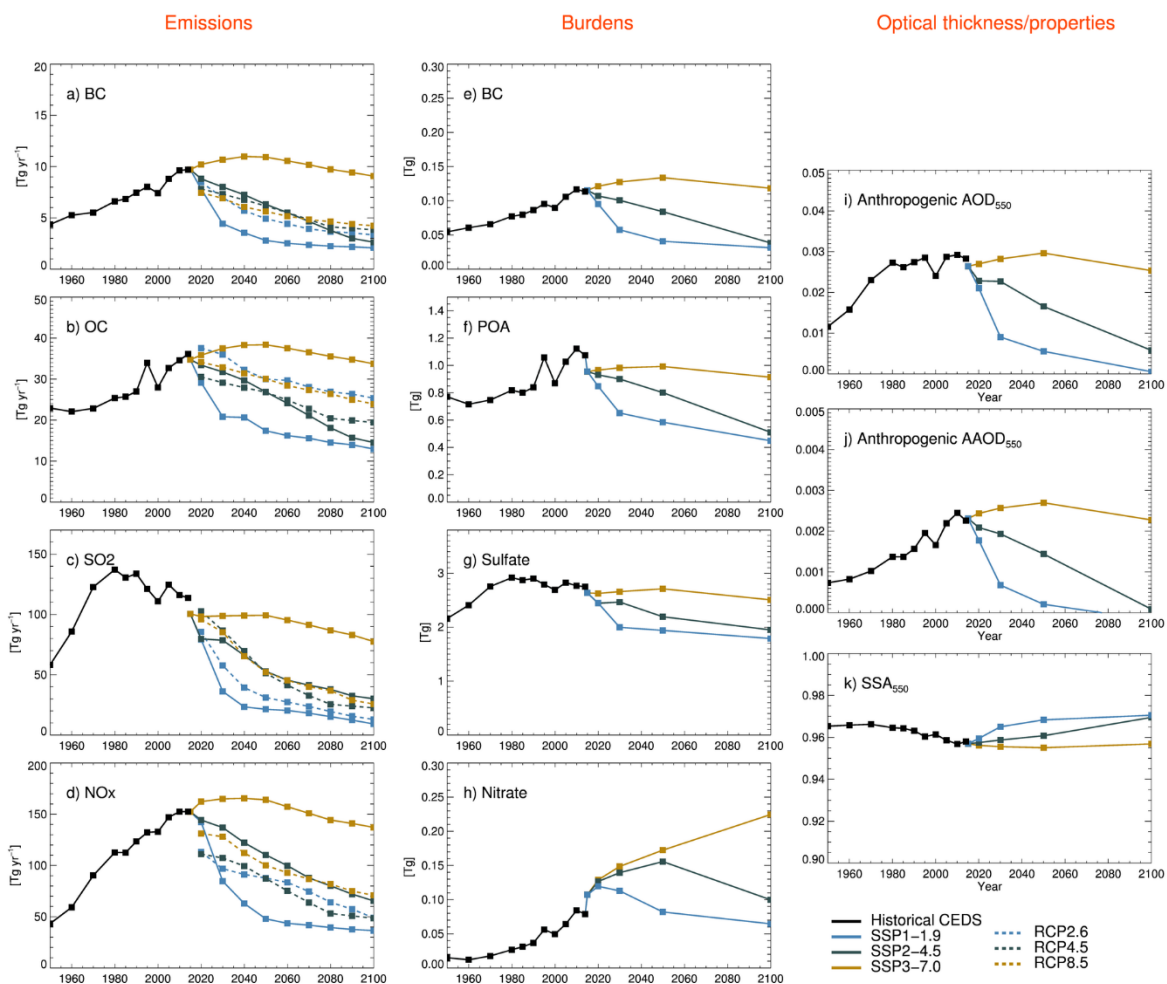
701 Westervelt D. M., Horowitz L. W., Naik V., Golaz J. C. & Mauzerall D. L.: Radiative  
702 forcing and climate response to projected 21st century aerosol decreases, *Atmos. Chem. Phys.*  
703 15(22), 12681-12703, 10.5194/acp-15-12681-2015, 2015.

704 Zheng B., Tong D., Li M., Liu F., Hong C., Geng G., Li H., Li X., Peng L., Qi J., Yan L.,  
705 Zhang Y., Zhao H., Zheng Y., He K. & Zhang Q.: Trends in China's anthropogenic emissions  
706 since 2010 as the consequence of clean air actions, *Atmos. Chem. Phys.* 18(19), 14095-14111,  
707 10.5194/acp-18-14095-2018, 2018.

708  
709  
710

711

712 Figures



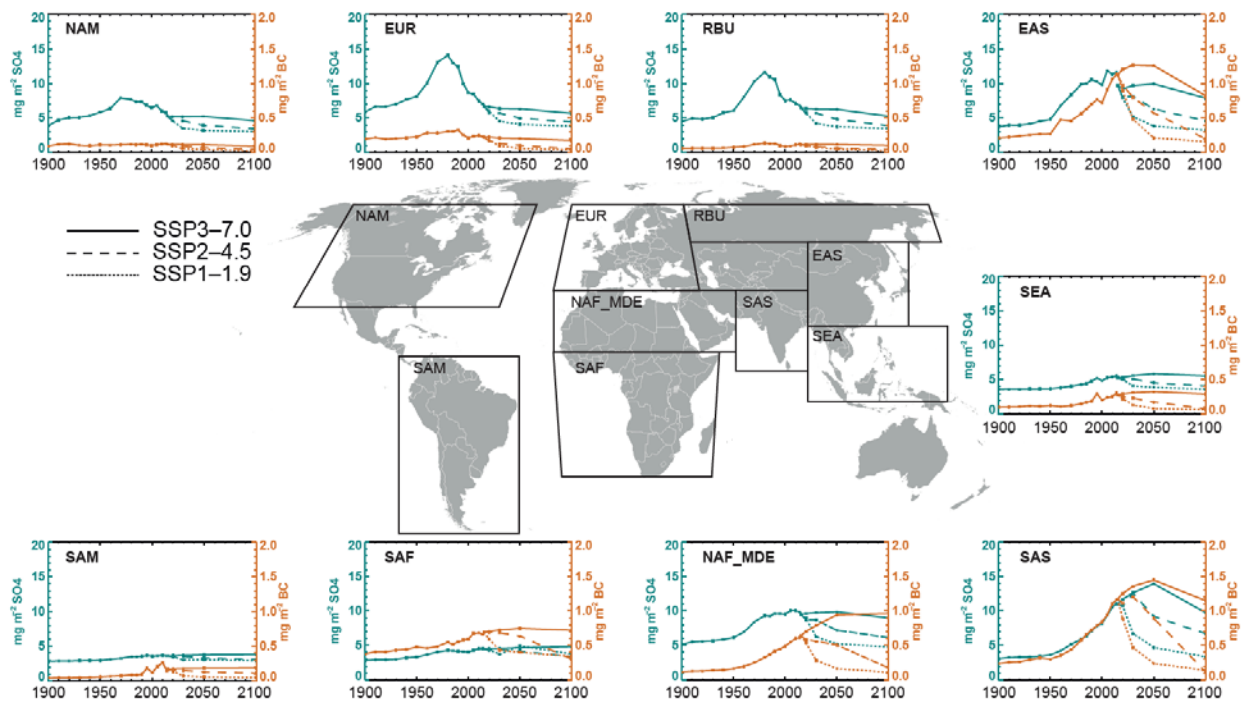
713

714 *Figure 1. Left: Annual global emissions (fossil fuel, biofuel and biomass burning) of BC, OC, SO<sub>2</sub> and NO<sub>x</sub>*  
715 *over the period 1950 to 2100 from the CEDS historical inventory and SSP1-1.9, SSP2-4.5 and SSP3-7.0*  
716 *(solid colored lines). Emissions from RCP2.6, RCP4.5 and RCP8.5 (dashed lines) are added for*  
717 *comparison. Middle: Modeled total global burdens of BC, POA, sulfate and fine mode nitrate. Right:*  
718 *Anthropogenic AOD and AAOD, and total (anthropogenic and natural) SSA at 550nm.*

719

720

721

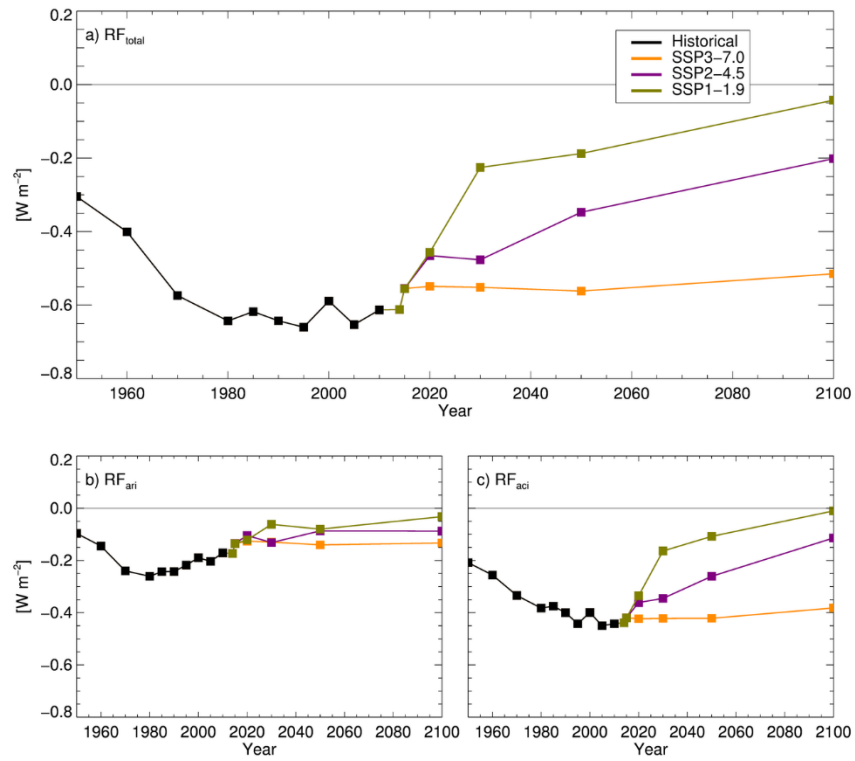


722

723 *Figure 2: Regionally averaged burdens of BC and sulfate aerosols from 1900 to 2100 using CEDS*  
 724 *historical emissions and SSP1-1.9, SSP2-4.5 and SSP3-7.0.*

725

726



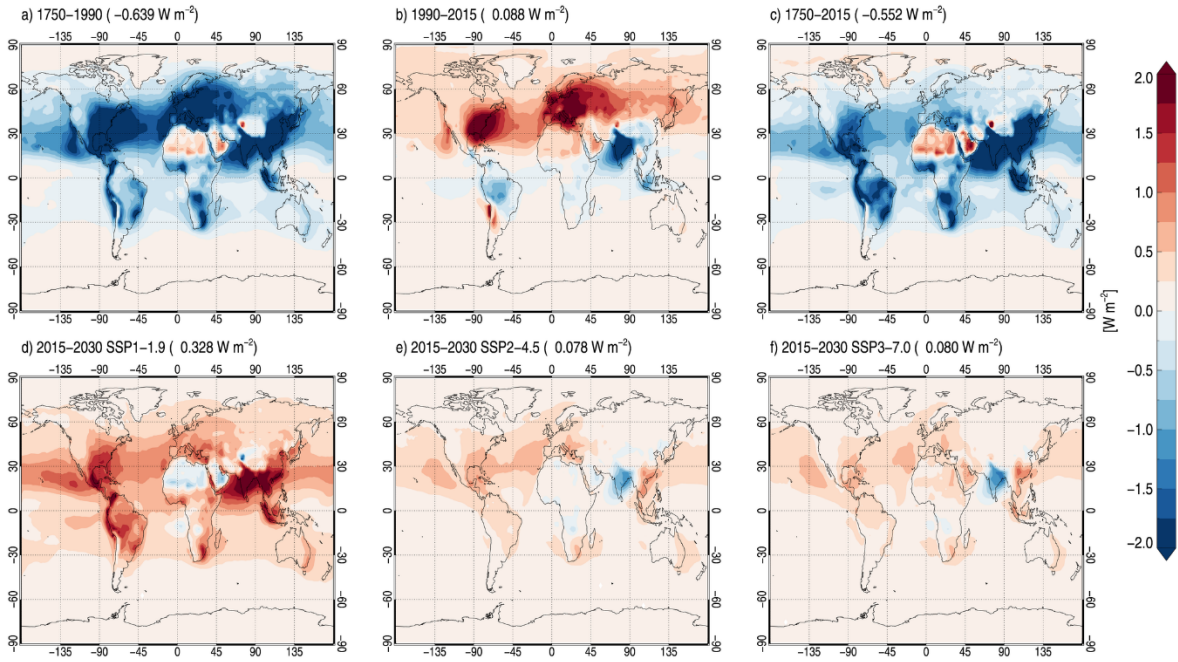
727

728 *Figure 3: Radiative forcing of anthropogenic aerosol 1950-2100 relative to 1750: a) total aerosol RF*  
 729 *( $RF_{total}$ ), b) aerosol-radiation interactions ( $RF_{ari}$ ) and c) aerosol-cloud interactions ( $RF_{aci}$ ).*

730

731

732



733

734 *Figure 4: Total aerosol RF over four time periods: 1750-1990, 1990-2015, 1750-2015, and 2015-2030 for*  
 735 *each of the three SSP scenarios considered here.*

736